Structurally Induced Supermodulus Effect in Superlattices

D. Wolf and J. F. Lutsko
Materials Science Division, Argonne National Laboratory, Argonne, Illinois 60439
(Received 16 November 1987)

It is suggested that the "supermodulus effect" observed for composition-modulated superlattices arises from the presence of the structurally disordered solid interfaces and not necessarily from electronic structure effects.

PACS numbers: 62.20.Dc, 61.70.Ng, 68.55.Pr

The discovery of the "supermodulus effect" in the biaxial modulus of composition-modulated structures of Au-Ni and Cu-Pd by Yang, Tsakalakos, and Hilliard[1] and its subsequent detection in a variety of metallic superlattice materials (see, for example, Schuller[2]) has drawn considerable attention to the possibility of designing interface materials with mechanical properties not otherwise achievable in bulk materials.

The elastic constants of an alloy usually show a behavior intermediate between those of its constituents. In the original work on Au-Ni and Cu-Pd the biaxial modulus in the interface plane was observed to be 2–3 times larger (for modulation wavelengths $\Lambda \approx 16$–20 Å) than for either of the constituents. Because of the severe difficulties encountered in the measurement of the elastic constants of thin-film materials, initially these experimental findings were met with some reservation. However, with the large number of different systems which have now been investigated and the variety of techniques utilized to study them, it is clear that "anomalous elastic behavior in metallic superlattices is the rule more than the exception."[3] Anomalous elastic properties have also been observed in nanocrystalline metals.[4] Considering their significantly lower density [with a large fraction of atoms situated in or near grain boundaries (GB's)], the recent observation[4] of elastic moduli which are nearly the same as (or even stronger than) those for conventional polycrystals also comes as a surprise.

In superlattice materials in which detailed x-ray studies exist (for overviews, see Refs. 2 and 3), the elastic anomalies are always accompanied by changes in interatomic spacings. In general, an expansion in the z direction (parallel to the plane normal) is observed which, in cases in which experiments were performed, is accompanied by a small contraction in the interface (x-y) plane. Whereas the latter can obviously explain the observed softening of the modulus for shear parallel to the interface plane,[5] the heart of the puzzle arises from the apparently parodoxial *strengthening* of the biaxial modulus in spite of a lattice *expansion* in z.

Essentially two qualitative explanations for these anomalies, both based on electronic structure arguments, have been proposed.[3,6] Remarkably, both models disregard any role the interfaces (as structural defects) might play, and hence predict the absence of such elastic-constant anomalies in grain-boundary materials. The anomalously high elastic constants of nanocrystalline Mg and Pd (Ref. 4) are obviously in conflict with both models. Instead, they seem to be indicative of an important role played by the structure, on an atomic scale, in the vicinity of the interface. The change in elastic properties would then be expected to be closely correlated with structural relaxations of the atoms in the interface region, and the effect would not be limited to dissimilar-material interfaces.

To study this question we have investigated, by means of computer-simulation methods, the elastic constants in what we call a "grain-boundary superlattice." Such a (somewhat hypothetical) material consists of a periodic arrangement, $\ldots |A|A'|A|A'| \ldots$, of thin slabs A and A' of equal thickness (see Fig. 1). In contrast to a composition-modulated alloy, however, A and A' consist of the same material (in our case, Cu) and are merely rotated with respect to each other about the z axis by a certain angle θ (between $A|A'$) or $-\theta$, respectively (between $A'|A$). Since much is known about the properties of grain boundaries on the (001) plane in the fcc structure we have chosen $z \| [001]$. In the terminology commonly used in the GB literature, A and A' are hence joined along a (001) twist boundary. For example, for $\theta = 36.87°$ about [001], the so-called $\Sigma 5$ (001) twist boundary is obtained. The area of the square unit cell of this coherent interface is $\Sigma = 5$ times that of the corresponding primitive planar unit cell ($\Sigma = 1$) on the (001)

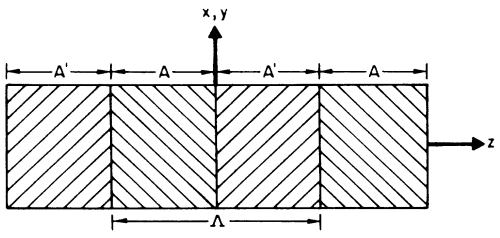

FIG. 1. Periodic arrangement of thin slabs A and A' to form a "grain-boundary superlattice." A and A' are slabs of the same material which were rotated about the plane normal ($\| z$) to form a periodic array of twist boundaries (x-y plane).

plane of an fcc crystal. The combination of this 2D periodic arrangement of atoms in the x-y plane with the periodic arrangement of interface planes in z (with modulation wavelength Λ) thus leads to a strictly 3D periodic atomic structure. We realize that by choosing such a GB superlattice we cannot attempt to reproduce any experimental observations on dissimilar-material superlattices. We hope to illustrate, however, that similar elastic-constant anomalies exist in both types of material.

Since virtually all elastic-property measurements mentioned above have been limited to rather low temperatures, an atomistic simulation code appropriate for $T=0$ studies has been used in our computer calculations. First, for a given value of Λ [i.e., for a given number of (001) planes in A and A'] the structure is relaxed under zero external stress. This so-called lattice-statics (iterative energy minimization) approach yields the fully relaxed atomic structure in which the forces on all atoms and all stresses on the unit cell vanish. The corresponding 6×6 elastic-constant and -compliance tensors at $T=0$ are then evaluated, from which all elastic moduli of interest can be extracted. Both an embedded-atom-method (EAM) potential[7] and a Lennard-Jones (LJ) potential for Cu used earlier[8] have been employed. The zero-temperature bulk ideal-crystal lattice parameters, a_0, associated with these shifted-force potentials were determined to be 3.6212 Å (EAM) and 3.6160 Å (LJ). In the principal cubic coordinate system (with x, y, $z\parallel\langle100\rangle$), the corresponding Young's moduli, Y_0, were found to be 3.30×10^{12} (EAM) and 1.09×10^{12} dyn/cm^2 (LJ) whereas the related shear moduli, G_0, are 2.20×10^{12} and 1.03×10^{12} dyn/cm^2. In the $\Lambda\rightarrow\infty$ limit, the average Young's modulus in the z direction, $Y_\infty=Y(\Lambda\rightarrow\infty)$, and the average shear modulus, $G_\infty=G(\Lambda\rightarrow\infty)$ {where $G(\Lambda)=[G_{xz}(\Lambda)+G_{yz}(\Lambda)]/2$}, for shear parallel to the interface plane are identical to Y_0 and G_0, respectively, since A and A' have been rotated about $z\parallel[001]$. Our results for $Y(\Lambda)$ and $G(\Lambda)$ obtained in the manner described above for the $\Sigma5$ boundary are summarized in Figs. 2 (EAM) and 3 (LJ). Shown also are the average lattice parameters, $\bar{a}_{xy}$ and $\bar{a}_z$, parallel and perpendicular to the interface plane. Notice that the moduli shown here are the ones which exhibit the largest anomalies and not necessarily the ones measured on dissimilar-materials superlattices.

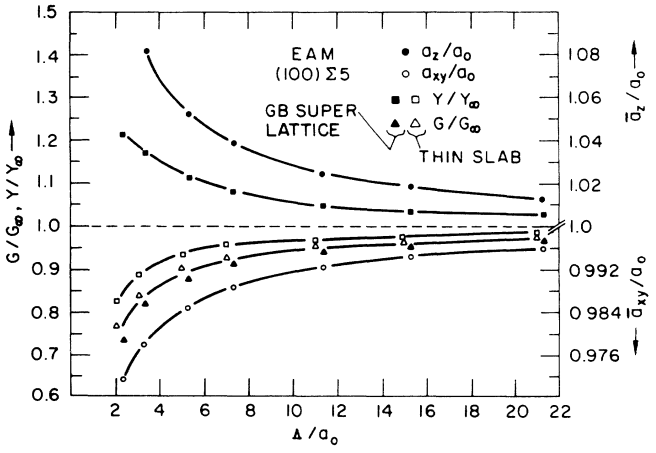

FIG. 2. Variation of Young's modulus parallel to the interface-plane normal and of the modulus for shear parallel to the interface plane as functions of Λ. Shown are results for the GB superlattice and for a thin ideal-crystal slab obtained by means of the EAM potential for Cu. Also shown are the *average* lattice parameters, $\bar{a}_z$ and $\bar{a}_{xy}$, for the superlattice (right-hand scales). The solid lines are merely a guide to the eye.

According to Figs. 2 and 3, both potentials yield an increase in Young's modulus and corresponding decrease in the shear modulus as Λ is decreased. Simultaneously, a substantial decrease in $\bar{a}_{xy}$ coupled with an even larger increase in $\bar{a}_z$ is observed. Results obtained for the $\Sigma29$ boundary on the (001) plane (for $\theta=43.60°$) are virtually identical to the ones in Figs. 2 and 3.

One might ask whether the Young's-modulus enhancement in the GB superlattice is truly an interface or merely a size effect; i.e., whether a thin slab of thickness Λ (containing no GB) shows the same behavior. The results obtained for such a fully relaxed slab are included in Figs. 2 and 3. Again, both EAM and LJ potentials yield the same qualitative behavior, namely a softening of both Young's and the shear moduli compared to their bulk values. This result is even more remarkable if we consider that the outermost (100) planes of the slab relax *outwards* for the LJ potential but *inwards* for the EAM potentials. We have also investigated a thin slab, $|A|A'|$, containing a single grain boundary for which moduli about halfway in between the ones for the thin slab and GB superlattice are obtained. We believe that this comparison demonstrates that the strengthening of Young's modulus arises from the presence of the interface.

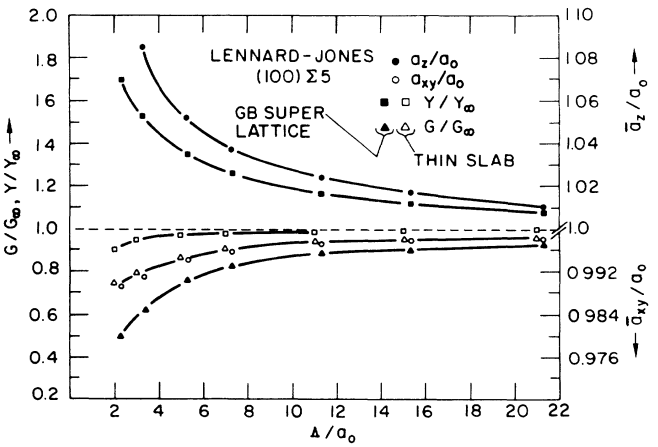

FIG. 3. Same as Fig. 2 for the Lennard-Jones potential for Cu (Ref 8). Notice that the scale on the left-hand side differs by a factor of 2 from the one in Fig. 2.

The contraction of $\bar{a}_{xy}$ is readily understood if we consider the substantial volume expansion in the z direction which results from the destruction of the perfect stacking of (001) planes at the interface. This not only leads to a substantial increase in $\bar{a}_z$ but, via the Poisson effect, to a decrease in $\bar{a}_{xy}$ and in the shear modulus. Another contribution to a decrease in the shear modulus arises from the very presence of the interface: Because of the destruction of the perfect stacking the two lattice planes facing each other across the GB plane are less perfectly locked into one another than in the perfect crystal, thus greatly facilitating a shear displacement parallel to the interface plane. The two contributions towards the shear-modulus decrease were investigated for the GB superlattice with the smallest value of Λ in Fig. 2. With suppression of any expansion in $\bar{a}_z$ the shear modulus is found to soften by about 10%, with an additional softening by about 15% if the expansion in z is allowed for.

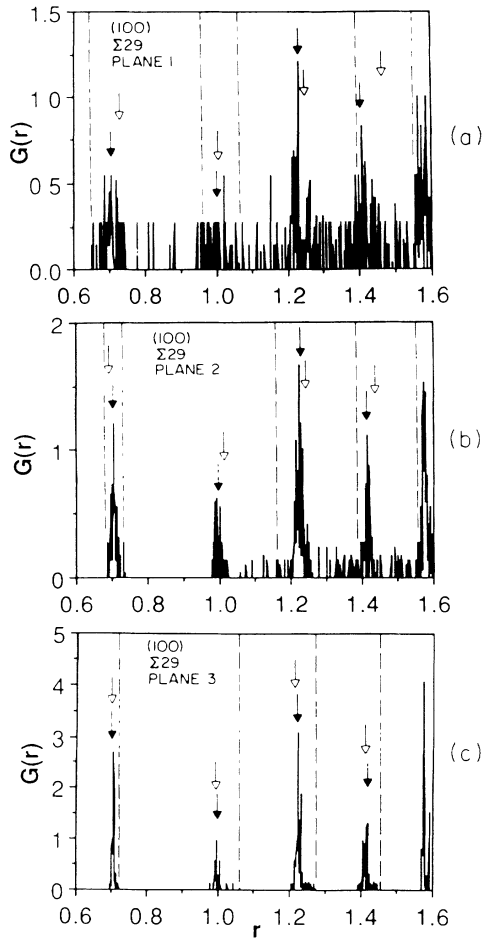

FIG. 4. Radial distribution functions, $G(r)$, for the three lattice planes nearest to the interface, obtained for the Σ29 GB superlattice for the largest $\Lambda(=21.27a_0)$. Full arrows indicate the corresponding perfect-crystal peak positions; open arrows show the average value of r in a given shell. The widths of these shells are indicated by the dashed lines. Whereas the atoms in the plane nearest to the interface (a) are very strongly affected by the presence of the interface, the atoms in the third-nearest plane (c) are found in an almost perfect-crystal environment.

The key question to be answered is this: How can the *increase* in $\bar{a}_z$ be accompanied by a parallel *increase* in Y? The answer is closely related to a general feature in the atomic structure of solid interfaces. Because of the destruction of the perfect-crystal planar stacking at the interface, atoms which were originally separated by perfect-crystal distances have been pushed together more closely. Essentially as a consequence of Pauli's principle, the bicrystal expands locally for all but very special geometries. As illustrated by the radial distribution functions in Figs. 4(a)–4(c) for the Σ29 boundary, however, in spite of the subsequent increase in the *average* interatomic distances (indicated by open arrows), especially in the lattice plane next to the interface (see Fig. 4(a)], a significant fraction of atoms is found at separations much shorter (up to about 10%) than in the perfect crystal. (For the case of grain boundaries it was demonstrated that these atoms are the ones governing the interface energy.[9,10]) As illustrated in Figs. 4(b) and 4(c), the fraction of atoms in non-ideal-crystal surroundings decreases very rapidly with increasing distance from the interface plane.

Within a given shell, distances shorter than the related ideal-crystal value (indicated by full arrows) are expected to strengthen the elastic constants whereas longer distances result in their softening. This effect is investigat-

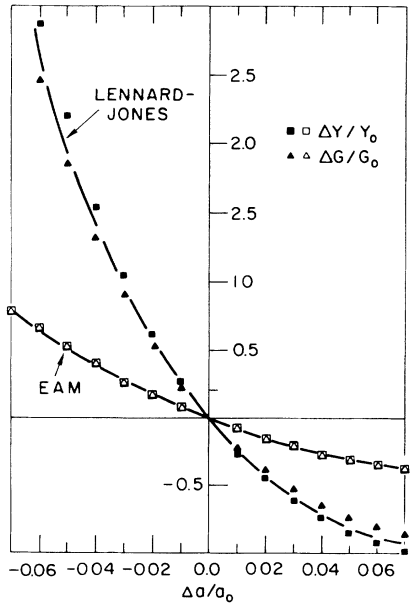

FIG. 5. Lattice-parameter dependence of the perfect-crystal Young's and shear moduli for both the EAM and LJ potentials. Y_0, G_0, and a_0 refer to the equilibrium values (at $T=0$) of Young's modulus, the shear modulus, and the lattice parameter, respectively. The solid lines are merely a guide to the eye.

ed more quantitatively in Fig. 5 in which the variations of Young's and the shear moduli as functions of the bulk ideal-crystal lattice parameter are illustrated. Two features in Fig. 5 are particularly remarkable. First, the pronounced positive curvature of the curves obtained for both potentials indicates that, say, a 5% compression of a bulk ideal crystal leads to a much larger modulus *strengthing* than the *softening* obtained for a corresponding 5% expansion. Distances on the left of the related full arrows in Fig. 4(a) (and the corresponding modulus strengthening) are therefore weighted more heavily than the larger distances on the right (giving rise to a softening). Second, the effect is much less pronounced for the EAM than for the LJ potential. This explains the quantitative differences in the elastic-modulus anomalies exhibited by the two potentials (see Figs. 2 and 3).

The rapid convergence of the radial distribution function towards its ideal-crystal form with increasing distance from the interface [see Figs. 4(a)–4(c)] is expected to give rise to a similarly rapid approach of the local elastic constants and the average interplanar lattice spacing towards their corresponding ideal-crystal values. The latter, for example, decreases from $d=0.59a_0$ directly at the interface to $d=0.505a_0$ and $d=0.502a_0$, respectively, for the two subsequent planes. At a distance of about five planes the average interplanar spacing is practically indistinguishable from its ideal-crystal value, $d=0.5a_0$ for (110) planes in fcc.

We believe that the above reasoning demonstrates that in nanocrystalline materials the connection between the average lattice parameter (or density) and the elastic properties is considerably more complex than our intuition gained from homogeneous systems would suggest.[4] We also point out that the above explanation presented for elastic-constant anomalies of a GB superlattice does not rule out additional anomalies which might arise when materials with different electronic properties are brought into contact.

We have greatly benefitted from discussions with S. Phillpot and M. Grimsditch. This work was supported by the U.S. Department of Energy, Office of Basic Energy Sciences–Materials Sciences under Contract No. W-31-109-Eng-38.

[1]W. M. C. Yang, T. Tsakalakos, and J. E. Hilliard, J. Appl. Phys. **48**, 876 (1977).

[2]See, for example, I. K. Schuller, in *The Institute of Electrical and Electronics Engineers Ultrasonics Symposium, 1985* edited by B. R. McAvoy (IEEE, New York, 1985), p. 1093.

[3]M. Grimsditch, to be published.

[4]D. Korn, A. Morsch, R. Birringer, W. Arnold, and H. Gleiter, in Proceedings of the International Conference on Structure and Properties of Internal Interfaces, Lake Placid, New York, July 1987, (to be published).

[5]I. K. Schuller and A. Rahman, Phys. Rev. Lett. **50**, 1377 (1983).

[6]T. B. Wu, J. Appl. Phys. **53**, 5265 (1982).

[7]M. S. Daw and M. I. Baskes, Phys. Rev. B **29**, 6443 (1984).

[8]J. F. Lutsko, D. Wolf, and S. Yip, in Ref. 4.

[9]D. Wolf, Acta Metall. **32**, 245 (1984).

[10]D. Wolf, J. Phys. (Paris) Colloq. **C4**, C4-197 (1985).